Integrated microfluidic device for the separation, decomposition and detection of low molecular weight S-nitrosothiols

Gerson Duarte-Junior, Abdulghani Ismail, Sophie Griveau, Fanny d'Orlyé, José Alberto Fracassi da Silva, Wendell Coltro, Fethi Bedioui, Anne Varenne

▶ **To cite this version:**

Gerson Duarte-Junior, Abdulghani Ismail, Sophie Griveau, Fanny d'Orlyé, José Alberto Fracassi da Silva, et al.. Integrated microfluidic device for the separation, decomposition and detection of low molecular weight S-nitrosothiols. Analyst, 2019, 144 (1), pp.180-185. 10.1039/c8an00757h . hal-02159778

HAL Id: hal-02159778
https://hal.science/hal-02159778

Submitted on 19 Jun 2019

HAL is a multi-disciplinary open access archive for the deposit and dissemination of scientific research documents, whether they are published or not. The documents may come from teaching and research institutions in France or abroad, or from public or private research centers.

L'archive ouverte pluridisciplinaire **HAL**, est destinée au dépôt et à la diffusion de documents scientifiques de niveau recherche, publiés ou non, émanant des établissements d'enseignement et de recherche français ou étrangers, des laboratoires publics ou privés.

Integrated microfluidic device for the separation, decomposition and detection of low molecular weight S-nitrosothiols

Gerson F. Duarte-Junior[a,b], Abdulghani Ismail[a,] Sophie Griveau[a], Fanny d'Orlyé [a], José Alberto Fracassi da Silva[e], Wendell K. T. Coltro[b], Fethi Bedioui [a], Anne Varenne[a*]

[a] Chimie ParisTech, PSL Research University, INSERM 1022, CNRS 8258 , Paris Descartes, Unité de Technologies Chimiques et Biologiques pour la Santé, 75005 Paris, France

[b] Instituto de Química, Universidade Federal de Goiás, Campus Samambaia, Goiânia, GO, 74690-900, Brazil

[c] Instituto de Química, Universidade Estadual de Campinas, UNICAMP, Campinas, SP, 13083-970, Brazil

*Corresponding Author. (anne.varenne@chimieparistech.psl.eu)

Abstract

S-nitrosothiols (RSNOs) are considered as biological circulating stocks of nitric oxide (NO) that have many roles *in-vivo*. The variation of RSNOs proportion occurs in several diseases, which makes them potent biomarkers. The identification and quantitation of each RSNO is therefore important for biomedical studies. For now, miniaturized devices have been used to detect RSNOs, based on their total quantitation without a preceding separation step. This study reports on an original and integrated microdevice allowing for the successive separation of low molecular weight RSNOs, their decomposition under metal catalysis, and the quantitation by amperometric detection of the produced nitrite, leading to their quantitation in a single run. For this purpose, a commercial SU-8/Pyrex microfluidic system was coupled to a portable and wireless potentiostat. Different operating and running parameters were optimized to achieve the best analytical performance allowing for LODs of 20 μM. The simultaneous separation of S-nitrosoglutathione and S-nitrosocysteine was successfully obtained within 75 s.

36

Introduction

S-Nitrosothiols (RSNOs) are nitric oxide (NO) carrier molecules that play important roles in several physiological functions (vasodilatation and relaxation[1, 2], antiplatelet aggregation[3, 4], antimicrobial[5], regulation and signaling protein function[6]…) and pathological events (neurodegenerative diseases such as Parkinson and Alzheimer[7], apoptosis[8], chronic obstructive pulmonary disease[9], preeclampsia[10], diabetes[11]…). RSNOs can be divided into low molecular weight (LMW) and high molecular weight (HMW) RSNOs. Although there is no defined border in terms of molecular mass, it is common to use the term “low molecular weight” for peptides and aminoacid S-nitrosothiols (such as S-nitrosoglutathione (GSNO) and S-nitrosocysteine (CySNO)) and “high molecular weight” for s-nitrosylated proteins (such as S-nitrosoalbumin (AlbSNO) and S-nitrosohemoglobin (HbSNO)). RSNOs store, transport and release NO. They can also inter-exchange NO through transnitrosation reaction[13]. The variation of RSNOs concentration has been shown to occur in many diseases[12]. For all these reasons, the development of powerful methodologies for the simultaneous quantitation of all RSNOs in a biological sample is crucial.

Numerous methods have been developed for RSNOs analysis, based on direct or indirect detection. Examples of direct detection consist in the

separation of RSNOs from other species by capillary electrophoresis (CE) or liquid chromatography followed by mass spectrometric or spectrophotometric detection[14]. For example, the simultaneous separation of S-nitrosoglutathione (GSNO) and S-nitrosocysteine (CySNO) was performed by our group using conventional CE equipped with capacitively coupled contactless conductivity detection but in a conventional system[15]. In another work, the simultaneous separation of GSNO, GSH, glutathione sulfonic and sulfinic acid by CE coupled to mass spectrometry was obtained[14]. Most standard methods developed for RSNOs quantitation reported in the literature remain indirect. They are based on the detection of their decomposition products[16], through homolytic or heterolytic cleavage of S-NO bond generating NO or NO^+ leading finally to NO_2^-. These decomposition products are then detected by spectrophotometry, fluorimetry, electrochemistry or chemiluminescence [16, 17]. Various reagents have been used to decompose RSNOs, such as metal cations[18] (Hg^{2+}, Cu^+), light[19] and heat[20], leading to different decomposition products: NO is generated[18] if Cu^+, light or heat are employed, whereas nitrite is directly generated[18, 21] when Hg^{2+} or Ag^+ are used.

Nowadays, miniaturization in chemical analysis has become a powerful tool contributing to reduce the samples/reagents amount, analysis time and

waste generation. Such an approach can be beneficial for the quantitation of RSNOs. Indeed, our group has recently reported on the colorimetric analysis of RSNOs in a microfluidic paper-based anaytical device[22]. This system allowed to perform analysis of total RSNOs in plasma samples without any separation step. Other approaches were proposed by Hunter et al. for NO[23] and total RSNO detection[24] (after light decomposition) using a single PDMS microfluidic channel with amperometric detection. In all cases no separation of RSNOs occurred before detection in these miniaturized devices. Also, Gunasekara et al[25] used microchip capillary electrophoresis (MCE) with amperometric detection to separate a NO donor (DEA-NONOate or Proli-NONOate) from NO and nitrite in less than one minute. Tu et al.[26] used MCE with fluorescence detection to separate and detect NO, reduced glutathione (GSH) and cysteine (Cys). Herein we report the design and optimization of a single-run MCE analytical strategy allowing for the first time the simultaneous quantitation of two low molecular weight RSNOs (S-nitrosoglutathione and S-nitrosocysteine), thanks to the integration of successive electrokinetic separation, RSNO decomposition by Hg^{2+} to nitrite and nitrite quantitation by amperometry.

Experimental

Chemicals

All reagents were of analytical grade and used as received. L-arginine (ARG), 2-(N-morpholino) ethanesulfonic acid (MES), acetic acid (HAc), L-histidine (His), sodium tetraborate, Sodium Nitrite, N-acetyl-p-aminophenol (Paracetamol), Mercury(II) Chloride, EDTA, hydrochloric acid, sodium phosphate monobasic, sodium phosphate dibasic, L-cysteine (Cys) and reduced glutathione (GSH), were purchased from Sigma Aldrich (St. Louis, MO, USA). All aqueous solutions were made using ultra-pure water with a resistivity of 18.2 MΩ.cm from a Pure Lab Flex system (ELGA Labwater, France).

Synthesis of S-nitrosothiols

GSNO was synthesized as described elsewhere[27]. Briefly, an equimolar amount of nitrite was added to the equimolar amount of GSH and HCl. The resulting pure solid was rinsed once with 80% acetone, twice with 100% acetone and three times with diethyl ether and then stocked in the dark at 20 °C.

S-Nitrosocysteine (CySNO) was daily synthesized using the method described by Peterson and coworkers [28]. Briefly, solutions of 5 mM CysNO

were prepared by reacting cysteine with an equimolar concentration of nitrite in acidic medium (0.1 M HCl) in a dark flask to avoid light decomposition. After 5 min, more than 90% of cysteine was converted into CysNO. The solution was neutralized by 0.1 M PBS buffer (pH 7.4) containing 0.5 mM EDTA to prevent decomposition by trace metal cation contaminants.

Final concentrations of RSNOs were determined spectrophotometrically in aqueous solution at 335 nm (ε = 586 and 503 $M^{-1}\,cm^{-1}$ for GSNO and CysNO, respectively)[29].

Instrumentation

Electrophoretic experiments were performed using a SU-8/Pyrex microchips with integrated micro band platinum electrodes at the outlet end of the separation channel from Micrux Technologies (Oviedo, Spain) (MCE-SU8-Pt001T) (**Figure 1**). Only working (WE) and reference (RE) electrodes were used, with widths of 50 µm and 250 µm, respectively. The separation and injection channel length were 35 mm and 10 mm, respectively. The microchannels width and depth were 50 µm and 20 µm, respectively. A microfluidic platform (Oviedo, Spain) (MCE-HOLDER-DC02) was used to interface the microchip with the amperometric detector and the high voltage

source. The high voltage source was a programmable HVS448-3000V 8-channels high-voltage supply (LabSmith Inc., CA, USA) controlled by Sequence software v.1.165. Amperometric detection was performed by a modified model 9051, 2-channel, wireless, portable and electrically isolated potentiostat (Pinnacle Technology, Lawrence, KS. USA) operating in a two-electrode format at a 5 Hz sampling rate (gain=5 000 000 V/A, resolution= 30 fA). This potentiostat is isolated which eliminates interferences from the high voltage power supply system used for the separation. This potentiostat was controlled by Sirenia Acquisition Software v.1.7.6. The WE and RE were connected to the corresponding electrodes using the commercial chip holder.

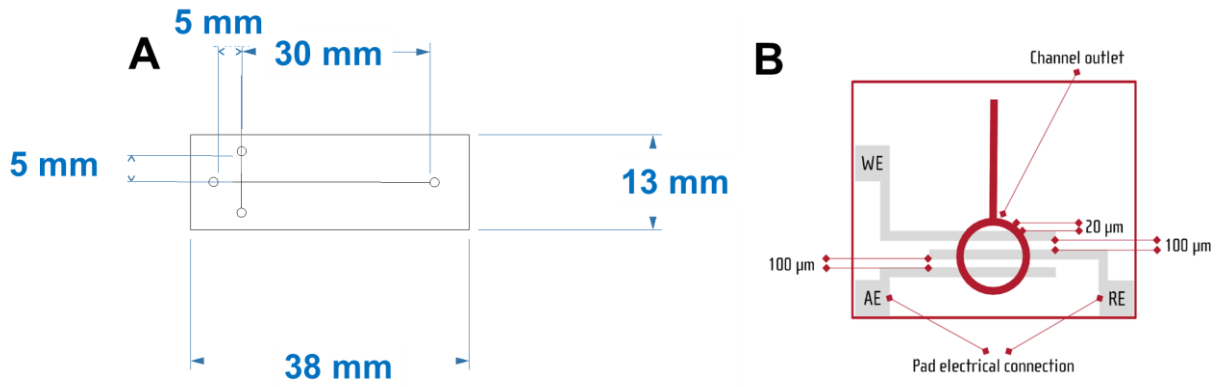

Figure 1 - Schematic presentation of A) dimensions and B) design of Micrux MCE-SU8-Pt001T chip. Adabpted from [30]

C^4D detection was performed using a commercial detector model ER815 acquired from eDAQ Pty (Denistone East, Australia). A microfluidic

platform EDAQ ET121 containing external electrodes was used to interface a commercial PMMA microchip (model 02-0750-0082-01, ChipShop, Jena, Netherlands) with the detection system. This microchip layout comprised separation and injection channels (50 μm wide/deep) with 87 and 10 mm long, respectively.

Electrophoresis and Decomposition procedure

Prior to analysis, microchannels were conditioned with 0.1 M NaOH, deionized water and running buffer. Samples of RSNOs and paracetamol (1 mM each) were electrokinetically injected by gated mode[31] by applying potentials of 800 V and 1000 V to sample and buffer reservoirs, respectively, while both waste reservoirs were grounded for the loading step. The injection was performed by floating the potential at the buffer reservoir for 3 s, giving the start of the separation step. The same procedure but under reversed polarity was performed for nitrite (1 mM) quantitation. For the decomposition step, $HgCl_2$ (10 mM) was added in the detection reservoir. Before RSNOs reach the buffer waste reservoir the polarity was inverted allowing detection of nitrite generated from decomposition. For amperometric detection of nitrite and paracetamol, potentials from 0.7 to 1.2 V *vs.* Pt were applied. Analysis using C^4D detection was realized under the same electrophoretic conditions and

detection was performed applying a sinusidal signal of 600 kHz and 90 $V_{peak\text{-}to\text{-}peak}$.

Results and discussion

Herein a method for successive separation, decomposition, and detection of RSNOs is proposed by integrating all the three steps in a microfluidic device. In order to achieve this goal, the decomposition should be *(i)* much faster than the separation process (otherwise the peaks originating from different RSNOs will overlap) *(ii)* quantitable and *(iii)* the decomposition product should be stable through the analysis time and operating conditions. It is well known that the decomposition product of RSNOs depends on the decomposition agent. As indicated above, the use of Cu^{+} or light leads to homolytic cleavage and to the formation of NO, while the use of Hg^{2+} leads to heterolytic cleavage and to the production of NO^{+} that transforms immediately to NO_2^{-}. Decomposition of RSNOs by light is slow (tenth of minutes are needed to decompose the sample[15]) and only partial decomposition of RSNOs have be obtained by Hunter et al[24] in a microfluidic device using 530 nm LED. Cu^{+} decomposition is faster than light decomposition but still insufficient (>2 min[32]) in comparison with the separation time scale. Moreover Cu^{+} is poorly soluble and stable in aquous solution and it is usually produced by reduction of Cu^{2+} with reducing agent such as GSH. Decomposition using Cu^{2+} is affected by the variation of GSH concentration in the sample, which is difficult to control [32]. Decomposition

using mercuric (II) is instantaneous leading to NO_2^- which is stable and electroacive[33]. Consequently, Hg^{2+} was chosen as the decomposition agent.

BGE plays an important role in the migration and electrochemical detection steps in micro chip electrophoresis (MCE) [34, 35]. As the objective was the detection of nitrite generated from RSNO decomposition, the BGE optimization was focused on nitrite signal/noise (S/N) ratio during detection. Several BGEs usually used for biological samples during MCE were tested : 20 mM MES / His (pH 6.0), 20 mM MES / Arg (pH 7.5), 20 mM Arg / Acetic Acid (pH 5.8). Nitrite (1 mM) was injected in the gated mode (see experimental section), separated and detected by amperometry using these various BGEs. For each BGE, the detection potential applied between WE and RE was varied from +0.5 V to +1.5 V keeping constant same electrophoretic injection and separation conditions. The optimal potential for nitrite detection in all BGE was 0.7 V. **Figure 2** shows electropherograms for the separation of nittire in various BGE. 20 mM MES/His (pH. 6.0) provided the highest amperometric detection signal. However, it was not selected for this design as Hg^{2+}, that will be used as the decomposition reagent for RSNO, reacts with histidine to form a precipitate. Although MES/Arg leads to the highest signal intensity, it however results in the

lowest signal to noise ratio. Therefore, the selected BGE, leading to the highest S/N ratio without interference with other molecules in the solution, was 20 mM Arg adjusted to pH 5.8 with HAc.

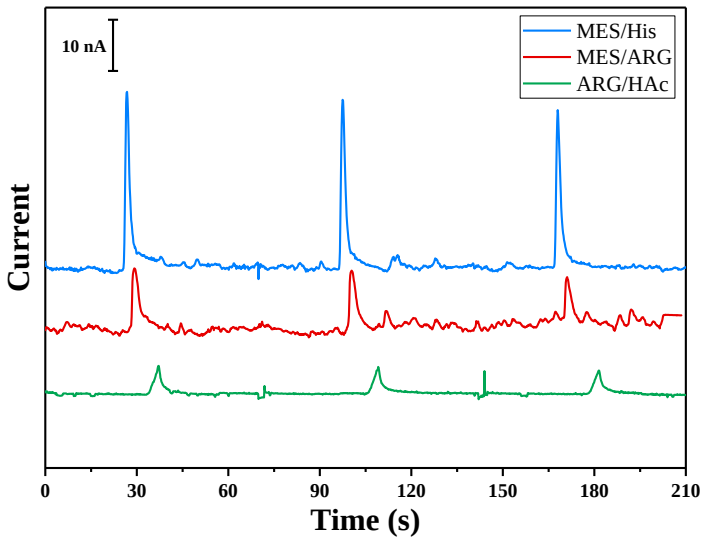

Figure 2 – Electrophoretic separation of 1 mM nitrite in SU-8/Pyrex microchip. BGE: MES (20 mM)/His (20 mM) pH 6.0 in blue, MES (20 mM)/ Arg (20 mM) pH 7.5 in red, Arg (20 mM) pH 5.8 adjusted with Acetic Acid in green. Gated injection V1=-800V, V2= -1000V, injection time 3s, successive injections: 70s, detection 0.7 V vs Pt.

For an optimized on-chip integration of the three steps involved in RSNOs characterization (separation, decomposition and detection) in the microchip, the apparent mobilities of each of the compounds (different RSNOs, nitrite, mercury) were determined. The overall procedure was first optimized for GSNO, as it is the most abundant low molecular weight RSNO. Control experiments by direct addition of nitrite into the BW reservoir, with or without application of electrophoretic voltage resulted in an amperometric

signal, proving the efficiency of the electrochemical detection step. A neutral electroactive marker (paracetamol) allowed determining the electroosmotic mobility as 1.85 ± 0.07 x10^{-4} $cm^2.V^{-1}.s^{-1}$ and GSNO electrophoretic mobility was determined as -0.64 ± 0.06 x10^{-4} $cm^2.V^{-1}.s^{-1}$, employing a C^4D detector, as GSNO is not electroactive (results not shown).

Under these experimental conditions, GSNO migrates towards the detector under a positive polarity. The device was primarily developed as follows: GSNO was electrokinetically injected from the sample reservoir (S) in the gated mode in positive polarity (see experimental section). Hg^{2+} was introduced in the waste reservoir (connected to the cathode) where it should decompose GSNO into nitrite upon reaching the buffer waste reservoir (BW). However, no amperometric signal was observed (results not shown). One hypothesis is based on the fact that Hg^{2+} undergoes diffusion from the BW within the separation channel, inducing the GSNO decomposition within the separation channel. As nitrite electrophoretic mobility under these experimental conditions (-4.25x10^{-4} $cm^2.V^{-1}.s^{-1}$) is higher in absolute value than the electroosmotic mobility, nitrite moves back to the sample reservoir (S) instead of the BW reservoir where it should be detected.

A new design was then developed, including an additional step allowing for voltage inversion just before GSNO decomposition (**Figure 3A).** In this new design, the loading, injection and separation steps were performed under positive polarity (step I, II and III, respectively), Hg^{2+} is added before GSNO reaches the channel end in step III, and polarity is inverted (step IV). This inversion of polarity leads to the migration of Hg^{2+} and GSNO to the sample reservoir (S). As Hg^{2+} migrates faster than GSNO, the migration zone of Hg^{2+} enters that of GSNO, allowing for GSNO decomposition. The produced nitrite migrates towards the BW reservoir and is detected (**see detail in step IV, Figure 3A**). A typical electropherogram obtained characterizing all the analytical steps is presented in **Figure. 3B.** Control experiments (without Hg^{2+} or without GSNO) did not show any signal (data not shown).

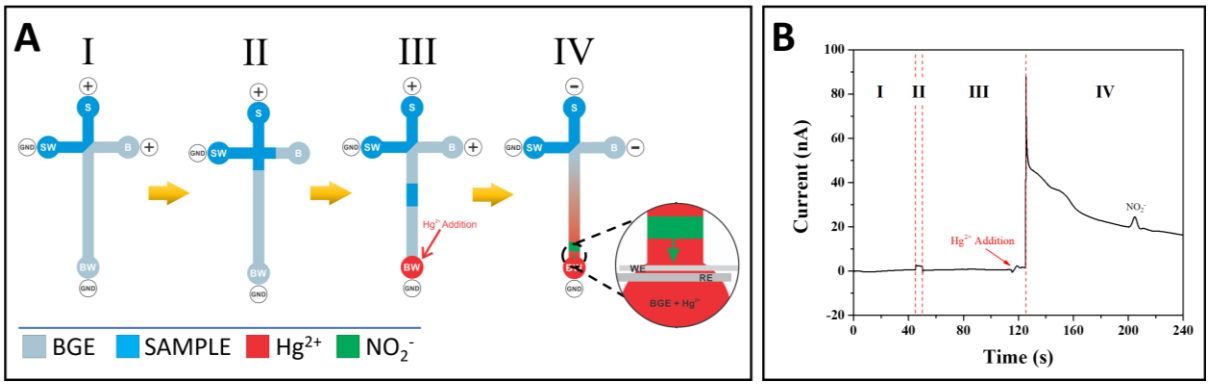

Figure 3 - (A) Scheme of the main steps for RSNOs quantitation. Loading step (I): Voltages of 800 and 1000 V are applied during 45 s to the sample (S) and buffer (B) reservoirs, respectively, grounding both waste reservoirs (SW and BW). Injection step (II): samples are injected into separation channel by floating the voltage applied to B reservoir during 3 s. Migration step (III): The potentials were then re-established to step I condition allowing the migration of RSNO sample towards separation channel. 15 s before the end of this step, Hg^{2+} was added to BW reservoir. Inversion and detection step (IV): In this

step the potential polarity is inverted which leads to the migration of Hg^{2+} into the separation channel faster than RSNO leading to RSNO decomposition. This is followed by nascent nitrite (in green) opposite migration towards the electrodes and detection by applying a potential of 1.2 V *vs Pt*. (B) Typical electropherogram obtained for GSNO (1 mmol/L) analysis characterising all the steps of the process.

Therefore, the overall integrated protocol includes (1) a separation of the RSNOs under positive polarity, (2) an inversion of the separation polarity, (3) a decomposition of RSNO thanks to the on-line crossing and mixing of RSNO and Hg^{2+} zones, respectively, due to different migration velocities, (4) the migration of the produced nitrite to the detector. So as to further optimize the experimental conditions to improve the limit of detection for nitrite, three parameters were studied; the BGE ionic strength (from 10 to 50 mM), the detection voltage (from 0.5 to 1.5 V *vs Pt*) and the time of polarity inversion. Considering the two first parameters, best signal intensities and S/N ratios for nitrite detection were obtained for a detection potential of 1.2 V (**Figure 4**).

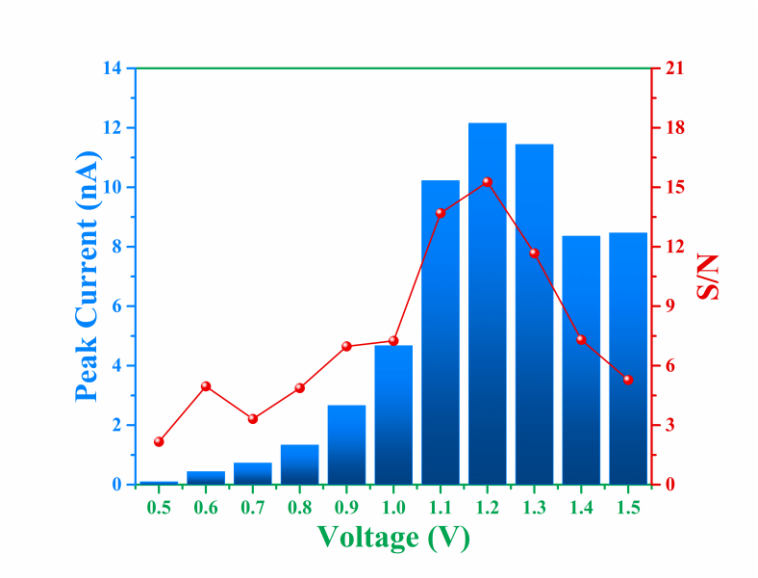

Figure 4 - Histogram of peak current (in nA) and signal-to-noise ratio (S/N) of nitrite (1 mM) injection in SU-8/Pyrex microchip obtained by variation of the detection potential from 0.5 to 1.5 V vs Pt. BGE: 20 mM arginine solution adjusted at pH 5.6 with acetic acid.

The time of polarity inversion is a crucial parameter as it should allow for the best separation of the RSNOs, their total decomposition and their optimal detection. For each studied compound, the electroosmotic and apparent mobilities must therefore be determined. For RSNOs of positive apparent mobility, the time of inversion should be chosen between the migration time of the neutral marker and the one of the RNSOs. This parameter was optimized for GSNO and CysNO. CysNO, another important nitrosothiol, as it is smaller than GSNO and with similar charge at this pH, presents a higher apparent mobility than GSNO. The best signal intensities were obtained for an inversion time of 90 s and 75 s, for GSNO and CysNO respectively (**Figure 5**). These results indicate the versatility of the

procedure for all types of RSNO. In these experimental conditions, the analytical performances of this methodology were determined for GSNO. The linearity was verified in the 100-700 µM concentration range (y=0.0485 x – 5.0485, R^2=0.9936) with a LOD of 20 µM

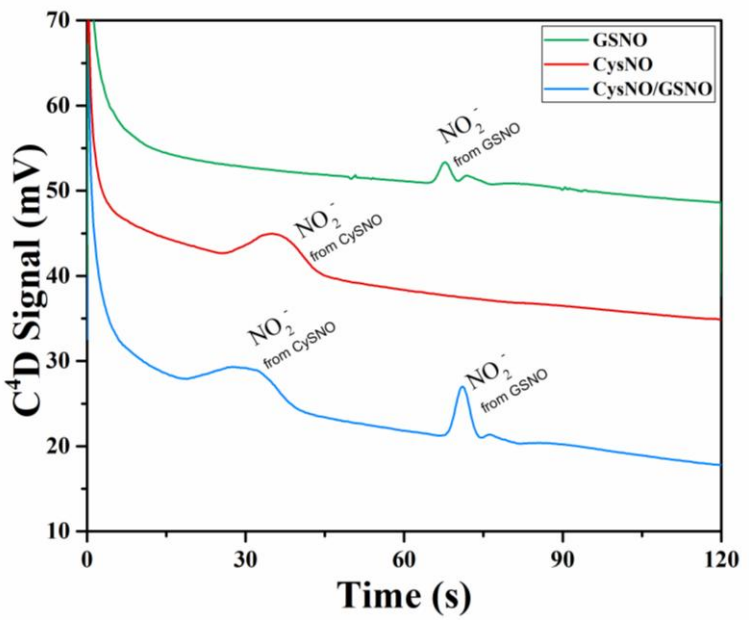

Figure 5 - Electropherograms for detection of 1 mM GSNO (Black) and 1 mM CySNO (Red and Blue) to determine the time of polarity inversion. In black and red 90 s was used for inversion while in blue 75 s. BGE: 20 mM arginine solution adjusted at pH 5.6 with acetic acid.

The final objective of such a micro-total analysis system is to allow for the simultaneous quantitation of various RSNOs. Therefore three main challenges have to be adressed : *(i)* the efficient separation of the different RSNOs, *(ii)* the choice of a unique time of polarity inversion in the process, and *(iii)* the efficient detection of the sucessive nitrite zones produced from each RSNOs decomposition.

315 The simultaneous separation of GSNO and CysNO was performed so as to
316 prove the versatility of the sytem. For this purpose, GSNO and CysNO were
317 first separated and detected individually. The crucial parameter being the
318 inversion time, different values were applied from 75 to 90 s. In a second
319 step, an equimolar mixture of CySNO and GSNO (1 mM each) was
320 separated and detected. **Figure 6** presents the resulting electropherograms
321 for an optimized inversion time of 75 s that corresponds to the migration
322 time of CysNO. As expected the signal arising from GSNO appears after
323 the one of CysNO, as CysNO has a higher apparent mobility. These results
324 indicate a powerfull simultaneous separation and indirect detection of
325 GSNO and CysNO. The similar intensities for GSNO and CySNO, injected
326 at the same concentration indicate that decomposition efficiency is similar
327 in both cases. This method is therefore applicable for the quantitation of
328 pharmaceutical RSNOs, future drug candidates. Some work is in progress
329 for decreasing the LODs to reach biological concentrations (less than 16
330 µM[22]).

331

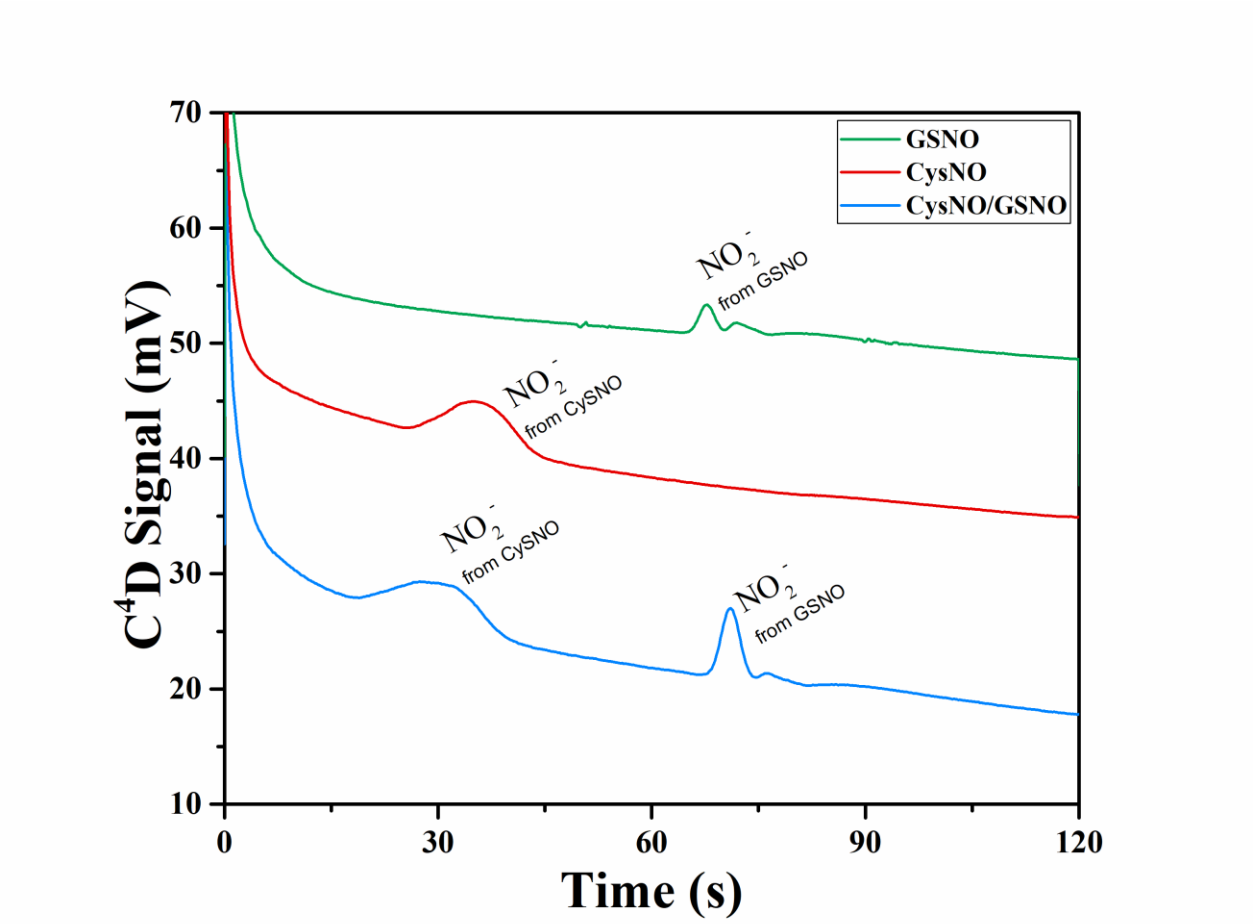

Figure 6 - Electropherograms corresponding to the electrophoretic profile of CySNO (1 mM), GSNO (1 mM) and mixture GSNO (1 mM) / CySNO (1 mM) in blue, red and black, respectively. Experiments were performed in Su-8/pyrex microchip with gated injection. Procedure : (1) 3s injection, (12) application of V1=800V, V2=1000V , during 3 minutes (not visible on the graph as it occurs before running the electropherogram), (3) addition of Hg^{2+} at t=0s of the electropherogram, and inversion of polarity V1=-800V, V2= -1000V for t=100s. Detection 1V vs Pt. BGE: ARG 20 mM adjusted to pH 5.8 with HAc

Conclusions

An original method to simultaneously quantify two low molecular RSNOs in a mixture using MCE was developed. A commercial microchip of SU-8/Pyrex microchip and a wireless isolated potentiostat were used. After the electrokinetic separation step, an inversion of electrokinetic polarity was necessary to mix the RSNOs with the decomposition agent within the separation channel and detect the produced nitrite by amperometric detection at the buffer waste reservoir. Optimization of BGE composition and detection potential were performed in order to obtain the best signal intensity and S/N ratio. The LODs were 20 µM for GSNO and CysNO. This methodology can be applied for the quantitation of pharmaceutical RSNOs, future drug candidates. Using a more environmental friendly decomposition reagent such as immobilized gold nanoparticles is envisaged. The method developed herein has shown to be versatile, opening the way to the quantitation of complex mixtures of RSNOs.

Conflicts of interest

The author declares no conflicts of interest.

Acknowledgements

Financial support from “Coordenação de Aperfeiçoamento de Pessoal de Nível Superior (CAPES)” and “French Committee for the Evaluation of Academic and Scientific Cooperation with Brazil (COFECUB)” (grant n° 802-14) is acknowledged.

References

1. B. T. Mellion, L. J. Ignarro, C. B. Myers, E. H. Ohlstein, B. A. Ballot, A. L. Hyman and P. J. Kadowitz, *Mol. Pharmacol.*, 1983, **23**, 653-664.
2. J. S. Stamler, D. I. Simon, J. A. Osborne, M. E. Mullins, O. Jaraki, T. Michel, D. J. Singel and J. Loscalzo, *Proc. Natl. Acad. Sci. U.S.A.*, 1992, **89**, 444-448.
3. E. J. Langford, A. S. Brown, R. J. Wainwright, A. J. Debelder, M. R. Thomas, R. E. A. Smith, M. W. Radomski, J. F. Martin and S. Moncada, *Lancet*, 1994, **344**, 1458-1460.
4. M. W. Radomski, D. D. Rees, A. Dutra and S. Moncada, *Br. J. Pharmacol.*, 1992, **107**, 745-749.
5. G. F. P. de Souza, J. K. U. Yokoyama-Yasunaka, A. B. Seabra, D. C. Miguel, M. G. de Oliveira and S. R. B. Uliana, *Nitric Oxide-Biol. Chem.*, 2006, **15**, 209-216.
6. C. G. Kevil and R. P. Patel, *Curr. Opin. Investig. Drugs*, 2010, **11**, 1127-1134.
7. M. Ito, *Annu. Rev. Neurosci.*, 1989, **12**, 85-102.
8. A. R. Butler and P. Rhodes, *Anal. Biochem.*, 1997, **249**, 1-9.
9. K. M. Beeh, J. Beier, N. Koppenhoefer and R. Buhl, *Chest*, 2004, **126**, 1116-1122.
10. V. A. Tyurin, S. X. Liu, Y. Y. Tyurina, N. B. Sussman, C. A. Hubel, J. M. Roberts, R. Taylor and V. E. Kagan, *Circ. Res.*, 2001, **88**, 1210-1215.
11. A. B. Milsom, C. J. H. Jones, J. Goodfellow, M. P. Frenneaux, J. R. Peters and P. E. James, *Diabetologia*, 2002, **45**, 1515-1522.
12. M. W. Foster, T. J. McMahon and J. S. Stamler, *Trends Mol. Med.*, 2003, **9**, 160.
13. B. C. Smith and M. A. Marletta, *Curr. Opin. Chem. Biol.*, 2012, **16**, 498-506.
14. A. Ismail, F. d’Orlyé, S. Griveau, J. A. F. Da Silva, F. Bedioui and A. Varenne, *Anal. bioanal. chem.*, 2015, **407**, 6221-6226.
15. A. Ismail, F. d'Orlye, S. Griveau, F. Bedioui, A. Varenne and J. A. F. da Silva, *Electrophoresis*, 2015, **36**, 1982-1988.
16. S. Griveau and F. Bedioui, *Analyst*, 2013, **138**, 5173-5181.
17. D. Giustarini, A. Milzani, I. Dalle-Donne and R. Rossi, *J. Chromatogr. B*, 2007, **851**, 124-139.
18. D. L. H. Williams, *Acc. Chem. Res.*, 1999, **32**, 869-876.
19. M. M. Veleeparampil, U. K. Aravind and C. T. Aravindakumar, *adv. phys. chem.*, 2009, **2009**.
20. M. G. de Oliveira, S. M. Shishido, A. B. Seabra and N. H. Morgon, *J. Phys. Chem. A*, 2002, **106**, 8963-8970.

21. H. R. Swift and D. L. H. Williams, *J. Chem. Soc., Perkin Trans. 2*, 1997, 1933-1935.
22. A. Ismail, M. O. Araujo, C. L. S. Chagas, S. Griveau, F. D'Orlye, A. Varenne, F. Bedioui and W. K. T. Coltro, *Analyst*, 2016, **141**, 6314-6320.
23. R. A. Hunter, B. J. Privett, W. H. Henley, E. R. Breed, Z. Liang, R. Mittal, B. P. Yoseph, J. E. McDunn, E. M. Burd, C. M. Coopersmith, J. M. Ramsey and M. H. Schoenfisch, *Anal. Chem.*, 2013, **85**, 6066-6072.
24. R. A. Hunter and M. H. Schoenfisch, *Anal. Chem.*, 2015, **87**, 3171-3176.
25. D. B. Gunasekara, M. K. Hulvey, S. M. Lunte and J. A. F. da Silva, *Anal. Bioanal. Chem.*, 2012, **403**, 2377-2384.
26. F. Q. Tu, L. Y. Zhang, X. F. Guo, Z. X. Zhang, H. Wang and H. S. Zhang, *J. Chromatogr. A*, 2014, **1359**, 309-316.
27. J.-W. Yoo, G. Acharya and C. H. Lee, *Biomaterials*, 2009, **30**, 3978-3985.
28. L. A. Peterson, T. Wagener, H. Sies and W. Stahl, *Chem. Res. Toxicol.*, 2007, **20**, 721-723.
29. R. A. Hunter and M. H. Schoenfisch, *Anal. Chem.*, 2015, **87**, 3171-3176.
30. https://www.micruxfluidic.com/en/ Acessed on 04/12/2018
31. S. C. Jacobson, S. V. Ermakov and J. M. Ramsey, *Anal. Chem.*, 1999, **71**, 3273-3276.
32. A. Ismail, S. Griveau, F. d'Orlyé, A. Varenne and F. Bedioui, *Electroanalysis*, 2015, **27**, 2857-2863.
33. B. Thirumalraj, S. Palanisamy, S.-M. Chen and D.-H. Zhao, *J. Colloid Interface Sci.*, 2016, **478**, 413-420.
34. P. Kubáň and P. C. Hauser, *Electrophoresis*, 2009, **30**, 3305-3314.
35. J. L. Beckers and P. Boček, *Electrophoresis*, 2003, **24**, 518-535.